文章编号：1001－9014(2017)03－0276－05

DOI:10.11972/j.issn.1001－9014.2017.03.005

Temperature-dependent optical properties of AlN films characterized by spectroscopic ellipsometry

LIN Shu-Yu[1], WU Feng[2], CHEN Chang-Qing[2], LIANG Yi[1*], WAN Ling-Yu[1*], FENG Zhe-Chuan[1]

(1. Laboratory of optoelectronic materials & detection technology, Guangxi Key Laboratory for Relativistic Astrophysics, College of Physics Science & Technology, Guangxi University, 530004 Nanning, China;
2. Wuhan National Laboratory for Optoelectronics, Huazhong University of Science and Technology, Wuhan 430074, China)

Abstract: We investigated the optical properties of AlN films with different thicknesses grown on sapphire by spectroscopic ellipsometry at different temperature. Based on a Tauc-Lorentz dispersion model, thickness and optical constants (the refractive index n, the extinction coefficient k) of AlN films were extracted by fitting the experimental data. Our results show that the refractive index of thicker AlN film possesses bigger values. Similar to the previous report, it was also found that the refractive index, the extinction coefficient and band gap of AlN films shift monotonously to lower energies (a redshift) with temperature increasing. Moreover, with rising temperature, varying the thicknesses of the films exhibits little influence on the shrinkage of bandgap but slight influence on the changes of the refractive index.

Key words: AlN, Spectroscopic Ellipsometry, thickness, temperature
PACS: 68.35.bg, 77.55.hd, 68.55.jd, 74.25.Gz

使用椭偏光谱研究氮化铝薄膜在不同温度下的光学性质

林书玉[1], 吴 峰[2], 陈长清[2], 梁 毅[1*], 万玲玉[1*], 冯哲川[1]

(1. 广西大学 物理科学与工程技术学院,广西相对论天体物理重点实验室,光电子材料与探测技术实验室,广西 南宁 530004;
2. 华中科技大学 武汉光电国家实验室,湖北 武汉 430074)

摘要:通过椭偏仪对生长在蓝宝石上的不同厚度氮化铝薄膜的变温光学性质进行了研究,并采用托克-洛伦兹模型对椭偏实验数据进行了拟合分析,精确得到了氮化铝薄膜的厚度和光学常数(折射率 n,消光系数 k)等.研究的结果表明:相比薄的氮化铝薄膜,厚的氮化铝薄膜的折射率较大.随着温度的升高,氮化铝的折射率、消光系数和带隙会向低能端单调地移动(红移);厚度对带隙随温度改变的影响较小,对折射率则有一定的影响.

关 键 词:氮化铝;椭偏仪;厚度;温度

中图分类号:O433.1,O433.4　　**文献标识码**:A

Introduction

Among the family of III-V direct-band-gap nitride semiconductors, aluminum nitride (AlN) has attracted a lot of attentions because of its wide band gap (6.2 eV) at room temperature. AlN exhibits high temperature stability, high hardness, high values of surface acoustic velocity, high thermal conductivity, high dielectric constant and so on[1-3]. These features, which distinguish AlN from other III-nitrides materials, have inspired many potential applications such as light-emitting devices in the ultraviolet and visible region, surface acoustic waves devices[4], piezoelectric sensors and actuators[5], anti-reflection layer on the solar coatings[6-7]. Therefore, it is very vital to conduct structural and optical analysis to un-

Received date: 2016-08-12, **revised date**: 2016-11-15　　**收稿日期**:2016-08-12, **修回日期**:2016-11-15
Foundation items: National Natural Science Foundation of China (61367004, 11604058), Guangxi Key Laboratory for Relativistic Astrophysics-Guangxi Natural Science Creative Team funding (2013GXNSFFA019001), Guangxi Natural Science Foundation (2016GXNSFBA380244)
Biography: LIN Shu-Yu (1993-), male, Guangxi, China, Master. Research fields focus on optoelectronic materials & detection teachnology. E-mail: linshuyu.123@foxmail.com
* **Corresponding author**: E-mail: liangyi@gxu.edu.cn, wanlingyu75@126.com

derstand the underlying mechanism of the properties of various AlN materials. Recently, thermal stability and thickness dependence of the refractive index and optical bandgap of AlN were investigated[8-9]. However, thickness effect on the optical properties of AlN film at variable temperature still lacks detailed study.

Spectroscopic ellipsometry (SE) is considered as one of the most powerful characterization techniques to obtain the information of optical properties of III-N semiconductor materials. Specially, SE technique are utilized to evaluate the materials dielectric functions $\varepsilon(E)$ including refractive indices and absorption coefficients of semiconductors, which is essential for the designs and analyses of the hetero-structure-based lasers and other waveguiding devices. In this paper, temperature-dependent spectroscopic ellipsometry (SE) was used to study the refractive index and absorption coefficient of AlN films with different thicknesses grown on sapphire substrate by metalorganic chemical vapor deposition (MOCVD). It was found that the refraction index and the absorption coefficient of AlN films decrease and redshift with rising temperature. Especially, the changes of optical constants (n) of the thicker AlN film at variable temperature are more obvious. To demonstrate this, Tauc-Lorentz dispersion model was employed to fit the SE spectra and the theoretical fit is in good agreement with the associated experimental observations.

1 Experiments

Our experiments were performed on two pieces of AlN samples labeled as AlN01 and AlN02, which were grown on c-plane sapphire substrate by metalorganic chemical vapor deposition (MOCVD). The growth pressure, temperature and source flow were 40 Torr, 1120℃ and 3090 sccm, respectively. The growth time of AlN 01 and AlN 02 are 40 min and 45 min, respectively. Then, at room temperature (RT), a dual rotating-compensator Mueller matrix ellipsometer (ME-L ellipsometer, Wuhan Eoptics Technology Co. Ltd., China) was used to performed the SE at an incident light angle of 50° and 55° (considering the optical anisotropy of the AlN films[2], the SE at two angles should be measured) in the range from 195 to 1695 nm (0.73 eV to 6.35 eV). The parameters including amplitude ratio Psi (Ψ) and phase difference Delta (Δ), which were used for the direct determination of material properties under certain conditions, e.g., optical constants (both n and k), were recorded as a function of the wavelength λ. Next, we repeated the same process to perform the spectroscopic ellipsometry measurements on these two AlN samples at variable temperature (VT) from 30℃ to 600℃. In this case, a Linkam THMS600 heating and cooling stage was used, where high heating/cooling rates with 0.01℃ accuracy and stability were realized.

2 Theory

Here, the fitting structural model used for the samples can be constructed as: Sapphire substrate // AlN buffer layer //AlN layer // surface roughness. Based on this structure, a Tauc-Lorentz mode was used to extract the complex dielectric function of AlN. The imaginary part of the dielectric function above the band edge from Tauc-Lorentz model is given as below[10-11]:

$$\varepsilon_2(E)\begin{cases}=\dfrac{AE_0C(E-E_g)^2}{(E^2-E_0^2)^2}\times\dfrac{1}{E}, E>E_g\\ =0, E\leqslant E_g\end{cases}, \quad (1)$$

where the four fitting parameters are the optical band gap E_g, the fitting constant A, the peak transition energy E_0, and the broadening term C, and all are in units of energy. Equation (1) is efficient for evaluating the dielectric function ε (or n, k) of direct bandgap semiconductors such as AlN.

The real part of the dielectric function ε_1 is obtained by exploiting the Kramers-Kronig integrations, i.e.

$$\varepsilon_1(E)=\varepsilon_1(\infty)+\frac{2}{\pi}P\int_{E_g}^{\infty}\frac{\xi\varepsilon_2(\xi)}{\xi^2-E^2}\mathrm{d}\varepsilon. \quad (2)$$

In Eq. (2), the term P stands for the Cauchy principal part of the integral and $\varepsilon_1(\infty)$ is added as a fitting parameter.

3 Results and discussion

3.1 SE analysis at room temperature

The SE results with different angles, i.e., the parameters including amplitude ratio Psi (Ψ) and phase difference Delta (Δ), are shown as a function of wavelength λ in Fig. 1, where solid lines depict experiment data and dotted lines are the fitting results. The fitting results agree well with the experimental data at different angles. Due to the effects of interference, several oscillation peaks appear in Fig. 1. These oscillation peaks are somewhat different for different thicknesses and incident angles. When the film becomes thicker, the interference is stronger, i.e. fewer oscillation peaks, as shown in Fig. 1(a) and (b). Obviously, the AlN film marked AlN01 is thinner than AlN02. Actually, from the fitting results, we have obtained their accurate structural parameters as follows: the film thicknesses of AlN01 and AlN02 are 778.0 nm and 2539.0 nm, respectively; the roughnesses of these two AlN samples are 2.994 nm for AlN01 and 2.170 nm for AlN02, respectively; buffer layer thicknesses are 1.03 nm for AlN01 and 1.0 nm for AlN02, respectively. Moreover, the peak transition energy E_0 of the films can be calculated, i.e. $E_0=6.528$ eV for AlN01 and $E_0=6.634$ eV for AlN02.

Figure 2 shows the fitted optical constant (n) as a function of photon energy E from Fig. 1. It is seen that these two samples have similar dispersion, except that the index of refraction peak position is 2.79 for AlN01 around 6.02 eV and 2.81 for AlN02 around 6.18 eV. It may be a result of more lattice mismatch-induced effects in a thinner film grown on sapphire substrate. In other words, thinner AlN film is grown with worse crystal orders and more defects, causing smaller band gap and peak refractive index. In general, there is influence of thickness on optical constants of thin AlN film, as mentioned in Ref. [9], wherein the refractive index varied with thickness at room temperature. However, this work has not reported thickness effect on optical properties of AlN film at variable temperature. So, next, we studied optical properties of AlN film by the temperature-depend-

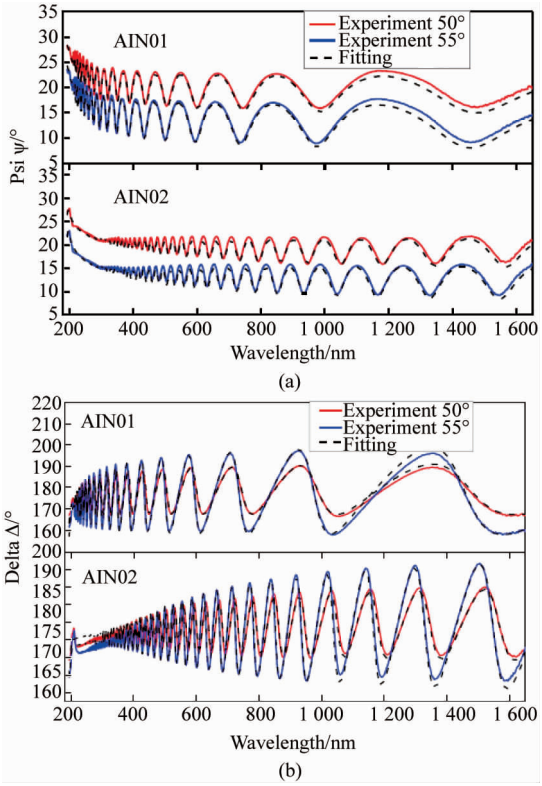

Fig. 1 SE experimental data and fitting results at room temperature, (a) Psi data, (b) Delta data

图1 室温下椭偏实验数据和拟合结果,图(a)Ψ数据,图(b)Δ数据

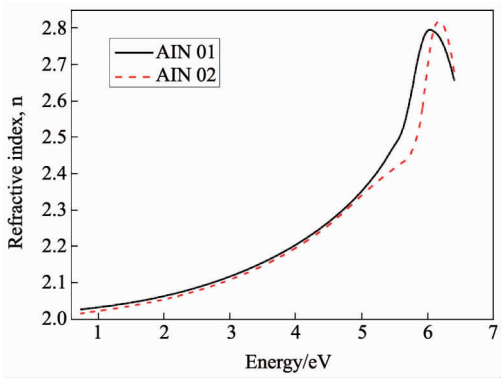

Fig. 2 Fitted optical constants (n) of AlN as a function of photon energy

图2 所拟合出的氮化铝光学常数(n)与能量的函数关系

ent spectroscopic ellipsometry.

3.2 SE analysis at variable temperature

The SE spectra of AlN film for AlN02 at variable temperature (30℃ to 600℃) are shown in Fig. 3, where (a) and (b) are refraction index and extinction coefficient as a function of the photon energy, respectively. In order to display the changes of optical constants (n, k) causing by temperature better, partly energy region amplification is depicted as an inset of Figs. 3(a) and (b). It is clearly to see that the refractive index and

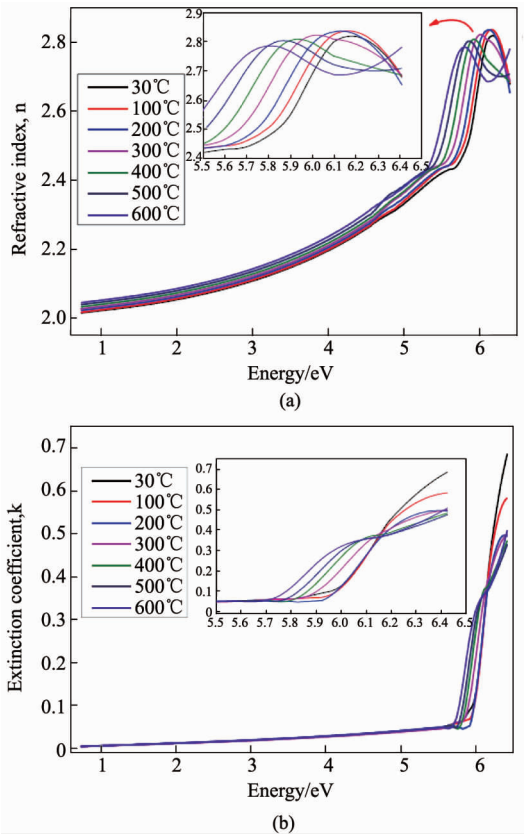

Fig. 3 Fitted optical constants (n and k) of AlN sample (02) with temperature varied from 30℃ to 600℃, (a) the refraction index (n), (b) the extinction coefficient (k)

图3 氮化铝样品(02)所拟合出的光学常数(n 和 k)与温度从30℃ 到600℃的关系,图(a)折射率(n),图(b)消光系数(k)

the extinction coefficient decrease and redshift when temperature increases. This interesting behavior is mainly contributed to variation of band gap with temperature, caused by lattice expansion and electron-phonon interaction. Usually, the band gap E_g can be expressed as a function of temperature by Varshni equation[12]:

$$E_g(T) = E(0) - \frac{aT^2}{T+\beta} \quad , \quad (3)$$

where $E(0)$ is the exciton energy at $T=0$ K, and a and β are fitting parameters. The relationship between the complex dielectric function and temperature can be given after substituting Eq. (3) back into Eq. (2). Thus, the refractive index and the extinction coefficient may be described as a function of temperature. When the band gap E_g decreases with increasing temperature, the refractive index and the extinction coefficient of AlN films decrease and redshift.

Figure 4 shows the $(\alpha h\upsilon)^2$ (α is the absorption coefficient and k is the extinction coefficient) versus energy of AlN films with temperature varied from 30℃ to 600℃. As one knows, the values of the bandgap (E_g) can be determined at the point of $(\alpha h\upsilon)^2=0$ by linear fit close to the absorption edge, as demonstrated in Figs. 4 ~ 5. Clearly, similar to the peaks of refractive index, the ab-

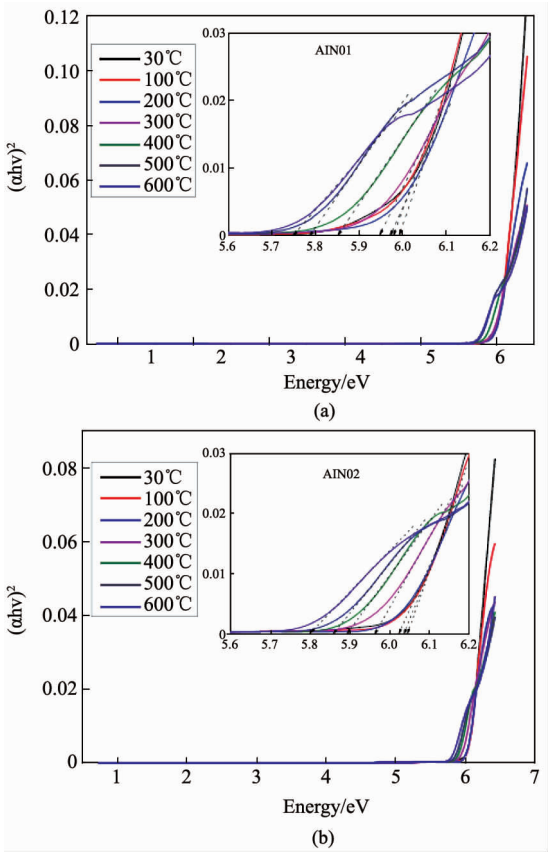

Fig. 4　The $(\alpha h\upsilon)^2$ vs energy of AlN with temperature varied from 30℃ to 600℃ for different samples
图 4　不同的两片氮化铝样品随温度从 30℃到 600℃的 $(\alpha h\upsilon)^2$ 与能量的关系图

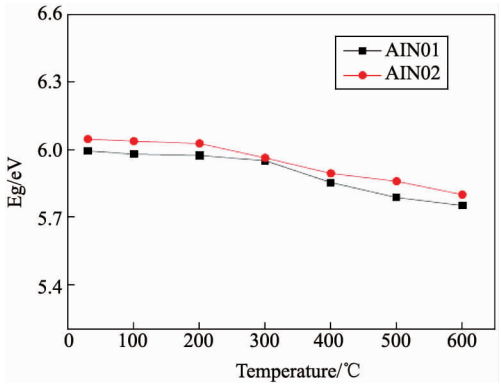

Fig. 5　E_g of AlN as a function of photon energy in different temperature
图 5　两片氮化铝样品带隙随温度的变化曲线

sorption edge also shifts to the lower energy (red-shift) with rising temperature. In other words, the bandgap redshifts when temperature increases (Fig. 5), which is in good agreement with Eq. (3). Here, the bandgap shrinkage with increasing temperature is contributed to two factors[3]: the change in bond length on the basis of lattice thermal expansion, and the change in electron-phonon interactions. These two factors give rise to a change of the energy of electronic transitions, resulting in the reduction of band gap. From Fig. 5, it is also found that, while temperature increases, the reductions of band gaps are similar for these two AlN samples, which means that thickness has little influence on the variation of bang-gap with temperature. However, because of worse crystal orders and more crystal defects (inducing intermediate energy levels that merge with the conduction band, and lower the band gap), thinner AlN film (AlN01) always presents a smaller band bap at each temperature point from 30℃ to 600℃, corresponding to the results in Ref. [9], i. e., dependence of optical band gap on thickness of AlN film. Then, according to Eqs. (1-2), the refractive index of thinner AlN film (AlN01) may cause a different variation with temperature from AlN02. To further prove this and investigate the effect of film thickness on optical properties of AlN, the SE measurement of AlN01 at variable temperature was also carried out. Comparing with AlN01, the refractive index of AlN02 changes more obviously (Fig. 6).

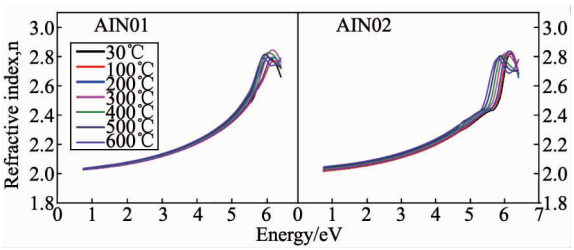

Fig. 6　Fitted optical constants (n) of AlN with temperature varied from 30℃ to 600℃ for two samples
图 6　两个氮化铝样品所拟合出的光学常数(n)随温度从 30℃到 600℃变化的关系

4　Conclusion

In summary, we have studied optical properties of AlN with different thicknesses on sapphire by metal organic chemical vapor deposition (MOCVD) via temperature-dependent spectroscopic ellipsometric technique. It was found that when the temperature increases, the refractive index, the extinction coefficient, and band gap of AlN film redshift. In addition, thinner AlN film always presents a smaller band bap at each temperature point even though the change of bandgap with temperature increasing is similar to the thicker film. Meanwhile, it seems like that the refractive index of thicker film changed more obviously with rising temperature. Our results may be useful for designing the high temperature stability devices based on AlN materials.

References

[1] XUE Jun-Shuai, HAO Yue, ZHANG Jin-Cheng, *et al*. Comparative study of different properties of GaN films grown on (0001) sapphire using high and low temperature AlN interlayers[J]. *Chin. Phys.* 2010, B(19): 057203.

[2] WEI Jiang, WEI Lin, LI Shu-Ping, *et al*. Optical anisotropy of AlN epilayer on sapphire substrate investigated by variable-angle spectroscopic ellipsometry [J]. *Optical Materials*, 2010, **32**: 891.

(下转第 301 页)

此外,界面态陷阱数量也大幅减小,有效提高了器件的稳定性.不同栅电压作用下器件反向特性出现了显著的变化,同时对器件 R_0A 也产生一定的影响.对标准工艺和改进工艺 B 制备的器件施加较大的正栅压后,器件 R_0A 减小,而采用改进工艺 C 制备的器件 R_0A 则未随栅压发生明显地变化.

致谢

笔者由衷地感谢红外探测器中心材料部为实验提供了高质量的 HgCdTe 薄膜样品,感谢器件部各工段在制备相关实验器件过程付出的辛勤努力和卓有成效的工作.

References

[1] Wenus J, Rutkowski J, Rogalski A. Surface leakage current in HgCdTe photodiodes [C]//*Proc. of SPIE*, 2002, **4650**: 250 - 258.

[2] Kumar V, Pal R, Chaudhury P K, *et al*. A CdTe passivation process for long wavelength infrared HgCdTe photo- detectors[J]. *Journal of Electronic Materials*, 2005, **34**(9): 1225 - 1229.

[3] Lee M Y, Lee H C. Novel surface treatment of HgCdTe using hydrazine[C]//*Proc. of SPIE*, 2004, **5406**: 821 - 828.

[4] Wang Ni-Li, Liu Shi-Jia, Lan Tian-Yi, *et al*. The Interfacial Properties of AOF/ZnS and LWIR Bulk HgCdTe Materials By MIS Structures [C]//*Proc. of SPIE*, 2012, **8419**: 84191D -1-84191D-5.

[5] Yuan Hao-Xin, Tong Fei-Ming, Tang Ding-Yuan. Electrical properties of p-type HgCdTe/ZnS interfaces[J]. *Optical Engineerin*, 1993, **32**: 608 - 612.

[6] Vishnu Gopal. Variable-area diode data analysis of surface and bulk effects in HgCdTe photo- detector arrays [J]. *Semicond. Sci. Technol*, 1994, **9**: 2267 - 2271.

[7] Xu Jing-Jie, Zhou Song-Min, Chen Xing-Guo, *et al*. Improvement of CdTe passivation by vacuum evaporation on HgCdTe infrared focal plane arrays [C]//*Proc. of SPIE*, 2012, **8419**: 84192D-1-84192D-6.

[8] Xie Xiao-Hui, Hua Hua, Qiu Guang-Yin, *et al*. Study of the Characteristics of VLWIR HgCdTe photovoltaic detectors in Variable-area Diode Test Structures [C]//*Proc. of SPIE*, 2011, **8193**: 819335-1-819335-7.

[9] Xie Xiao-Hui, Liao Qing-Jun, Zhu Jian-Mei, *et al*. Surface treatment effects on the I-V characteristics of HgCdTe LW Infrared photovoltaic detectors[C]//*Proc. of SPIE*, 2012, **8419**: 84191G-1-84191G-5.

[10] Dhar V, Bhan R K, Ashokan R, *et al*. Quasi-2D analysis of the effect of passivant on the performance of long-wavelength infrared HgCdTe photodiodes [J]. *Semicond. Sci. Technol*, 1996, **11**: 1302 - 1309.

[11] Rutkowski J, Wenus J, Gawron W, *et al*. Gate-controlled narrow band gap photodiodes passivated with RF sputtered dielectrics[C]// Opto-Electronics Review, 1999, **7**(2): 97 - 101.

[12] Kim Y H, Bae S H, Lee H C, *et al*. Surface leakage current analysis of ion implanted ZnS-Passivated n-on-p HgCdTe diodes in weak inversion [J]. *Journal of Electronic Materials*, 2000, **29**(6): 832 - 836.

[13] YING Ming-Jiong. Research of passivation technology of PV $Hg_{1-x}Cd_xTe$ surfaces: A two-layer combination of an anodic sulfidization with a deposited Zns[J]. *Laser&Infrared* (应明炯. 光伏碲镉汞表面钝化技术研究:用阳极硫化/硫化锌复合钝化碲镉汞表面. **激光与红外**), 1994, **23**(6): 33 - 36.

[14] YUAN Hao-Xin, TONG Fei-Ming, TANG Ding-Yuan. Experimental and theoretical investigations of surface channel leakage current in Hg_1-xCd_xTe N^+-P gate-controlled photodiodes [J]. *J. Infrared Millim. Waves* (袁皓心, 童斐明, 汤定元. $Hg_{1-x}Cd_xTe$ N^+-P 栅控二极管表面沟道漏电的理论和实验研究. **红外与毫米波学报**), 1992, **11**(1): 11 - 20.

[15] Kim J S, Song J H, Su S H. Electrical Properties of ZnS, CdTe/HgCdTe Interfaces Evaporated from Effusion Cell in UHV Chamber [C]//*Proc. of SPIE*, 2000, **4130**: 816 - 822.

[16] LI Xiong-Jun, HAN Fu-Zhong, LI Dong-Sheng, *et al*. A Study of Interface Electrical Characteristics for MW HgCdTe/ Passivation Layer[J]. *Infrared Technology*(李雄军,韩福忠,李东升,等. 中波碲镉汞/钝化层界面电学特性研究. **红外技术**), 2015, **37**(10): 868 - 872.

(上接第 279 页)

[3] FENG Zhe Chuan (ed.). III-Nitride Semiconductor Materials [M]. *London*: *Imperial College Press*, 2006, 422pp.

[4] Clement M, Vergara L, Sangrador J, Iborra E, *et al*. SAW character-istics of AlN films sputtered on silicon substrates [J]. *Ultrasonics*, 2004, **42**: 403.

[5] Bjurström J, Wingqvist G, Katardjiev I. Synthesis of textured thin piezo-electric AlN films with a nonzero c-axis mean tilt for the fabrication of shear mode resonators [J]. *IEEE Trans. Ultrason. Ferroelectr. Freq. Control*, 2006, **53**: 2095.

[6] ZhANG Qi-Chu, SHEN Y G. High performance W-AlN cermet solar coatings designedby modelling calculations and deposited by DC magnetron sputtering [J]. *Sol. Energy Mater. Sol. Cells*, 2004, **81**: 25.

[7] ZHAO Shu-Xi, Wäckelgård E. The optical properties of sputtered composite of Al-AlN[J]. *Sol. Energy Mater. Sol. Cells*, 2006, **90**(13): 1861.

[8] MENG Jian-Ping, LIU Xiao-Peng, FU Zhi-Qiang, *et al*. Thermal stability of AlN films prepared by ion beam assisted deposition [J]. *Applied Surface Science*, 2015, **347**: 109.

[9] Motamedi P, Cadien K. Structural and optical characterization of low-temperature ALD crystalline AlN [J]. *Journal of Crystal Growth*, 2015, **421**: 45.

[10] Blanckenhagen B. V, Tonova D. and Ullmann J. Application of the Tauc-Lorentz formulation to the interband absorption of optical coating materials. [J]. *Appl. Opt.*, 2002, **41**: 3137.

[11] Hilfiker J. N, Singh N, Tiwald T, *et al*. Survey of methods to characterize thin absorbing films with Spectroscopic Ellipsometry [J]. *Thin Solid Films*, 2008, **516**: 7979.

[12] Nepal N, Li J, Nakarmi M L, *et al*. Temperature and compositional dependence of the energy band gap of AlGaN alloys [J]. *Appl. Phys. Lett.*, 2005, **87**: 242104.